PCCP

Cite this: *Phys. Chem. Chem. Phys.*, 2011, **13**, 17852–17863

www.rsc.org/pccp

PAPER

Quantitative analysis of energy transfer between fluorescent proteins in CFP–GBP–YFP and its response to Ca^{2+} †

Christof Strohhöfer,*[a] Thilo Förster,[a] Dušan Chorvát,[bc] Peter Kasák,[c] Igor Lacík,[c] Marina Koukaki,[d] Spyridoula Karamanou[d] and Anastassios Economou[de]

Received 7th April 2011, Accepted 18th August 2011
DOI: 10.1039/c1cp21088b

This article reports the full characterisation of the optical properties of a biosynthesised protein consisting of fused cyan fluorescent protein, glucose binding protein and yellow fluorescent protein. The cyan and yellow fluorescent proteins act as donors and acceptors for intramolecular fluorescence resonance energy transfer. Absorption, fluorescence, excitation and fluorescence decays of the compound protein were measured and compared with those of free fluorescent proteins. Signatures of energy transfer were identified in the spectral intensities and fluorescence decays. A model describing the fluorescence properties including energy transfer in terms of rate equations is presented and all relevant parameters are extracted from the measurements. The compound protein changes conformation on binding with calcium ions. This is reflected in a change of energy transfer efficiency between the fluorescent proteins. We track the conformational change and the kinetics of the calcium binding reaction from fluorescence intensity and decay measurements and interpret the results in light of the rate equation model. This visualisation of change in protein conformation has the potential to serve as an analytical tool in the study of protein structure changes in real time, in the development of biosensor proteins and in characterizing protein–drug interactions.

Introduction

Discovery of the green fluorescent protein (GFP) and its spectral variants[1] opened a whole new dimension to biomedical research thanks to the proteins' ability to specifically label biomolecules and in this way to image and/or biochemically characterize structural and functional organization of the living cell.[2] This contribution was recognized with the 2008 Nobel Prize award in chemistry to Shimomura, Chalfie and Tsien. A wide spectrum of new emerging applications based on fluorescence proteins have been reported including in specific imaging of animal[3,4] and plant tissues[5] and subcellular locations,[6] tagging and isolation of cells,[7] directed evolution[8] and folding[9] of proteins and in both cell[10]- and protein[11]-based biosensors.[12,13] One of the most promising and interesting approaches is to monitor the fluorescence resonance energy transfer (FRET) between two fluorescent proteins.[14,15] FRET is a non-radiative transfer of energy from the donor—an excited fluorophore—to an acceptor molecule.[16] The energy transfer invokes changes in the fluorophores' optical properties, such as fluorescence intensity, spectral shape or excited state lifetimes.[17] FRET is used to visualize processes such as protein–protein interactions[18,19] and trafficking[20] *in vivo*, imaging of small molecule binding to proteins,[21] conformational dynamics of molecules[22] or sensing of the molecular environment.[23]

FRET-based molecular sensors follow a similar principle, linking an appropriate pair of fluorescent proteins to a molecular recognition domain. Conformation of the recognition domain is dependent on the environment and can be modulated by a specific trigger, such as binding of a ligand. Conformational change of the sensing domain alters the distance between the two fluorescent protein moieties, which is reflected in a change of their FRET efficiency. If the affinity of the sensing domain to the analyte is selected or adjusted properly, these FRET molecules form the foundation of a biosensor which can monitor analytes in real time without the need for additional reagents. This FRET signal varies with analyte concentration. Such molecules have been integrated into miniaturized biosensor systems.[24]

The large variety of available fluorescent proteins and chromophores, and their combination with proteins with

[a] *Fraunhofer EMFT, Hansastr. 27 D, München, Germany. E-mail: christof.strohhoefer@emft.fraunhofer.de; Fax: +49 89 54759 100; Tel: +49 89 54759 320*
[b] *International Laser Centre, Ilkovičova 3, Bratislava, Slovakia*
[c] *Polymer Institute, Dúbravská cesta 9, Bratislava, Slovakia*
[d] *Institute of Molecular Biology and Biotechnology, Foundation of Research and Technology—HELLAS, Iraklio, Crete, Greece*
[e] *Department of Biology, University of Crete, Iraklio, Crete, Greece*
† Electronic supplementary information (ESI) available: Construction of the proteins, detailed description of the optical measurements, detailed derivation of the kinetic model of protein fluorescence based on rate equations. See DOI: 10.1039/c1cp21088b

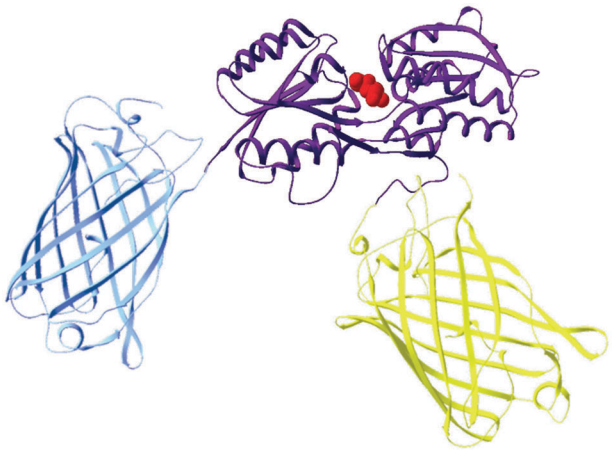

Fig. 1 Rendering of the FRET construct CFP–GBP–YFP used in this study. The structures of cyan fluorescent protein (pdb accession number: 2WSN), glucose–galactose binding protein from *E. coli* (pdb accession number: 2HPH) and yellow fluorescent protein (pdb accession number: 2YFP) are shown in ribbon representation. The three structures were assembled in a hypothetical representation to serve as a visual aid only. A glucose molecule (red; space filling model) is shown sandwiched between the two lobes of the glucose–galactose binding protein.

highly specific binding sites for relevant analytes by genetic engineering, leads to a large diversity of potential biosensor molecules.[13] Here, we evaluate FRET in a construct consisting of cyan and yellow fluorescent proteins (CFP and YFP, respectively) and a glucose binding protein (GBP) moiety that contains a binding site for a structural Ca^{2+} ion[25] (Fig. 1). We regard it as a representative FRET-based biosensor and aim to quantitatively describe its photophysical behavior.

FRET biosensors provide several ways to assess analyte binding and release. Here we combine steady-state spectroscopy with advanced spectrally-resolved fluorescence lifetime measurements, which provide optimal complementary information about energy transfer-related changes in the excited state kinetics of the fluorescent proteins in the FRET macromolecular construct.[26,27]

To have a tool at hand to quantitatively describe fluorescence and FRET of the proteins, we developed a suitable photophysical model based on rate equations.

Since CFP and YFP are separated by the large functional GBP domain, they interact only by Förster-type energy transfer. Therefore, we describe the individual fluorescent proteins as two-state systems, and the FRET protein as a linear combination of the photophysical properties of the donor and acceptor moieties. This model, although simple in view of the rather complex photophysical properties of CFP,[28,29] adequately describes both steady-state and time-resolved fluorescence data. Furthermore, the model provides insights into the energy transfer processes between CFP and YFP. The complete set of parameters of the model is extracted from the steady-state and time-resolved experiments. In this way, we achieve a full description of the photophysical behaviour of CFP–GBP–YFP.

CFP–GBP–YFP is ideally suited for the study of ligand–protein interactions, as its optical properties change markedly as a result of ligand binding, in this case Ca^{2+} ions. This kind of molecule provides two types of information: first, that a binding event has taken place, and second, that the sensor protein is undergoing structural changes. As this biosensor emits a strong optical signal and can immediately sense even minor conformational events within GBP, it is a very sensitive reporter of its conformational and ligand occupancy state. Ultimately, we use the model to monitor and interpret conformational change of CFP–GBP–YFP when it is binding or releasing Ca^{2+}.

Materials and methods

Proteins

Preparation of proteins is described in detail in the ESI.†

Steady state and time-resolved spectroscopy

Experimental methods used for measurement of absorption spectra as well as steady state and time-resolved fluorescence spectra are described in detail in the ESI.†

Kinetic model of protein fluorescence based on rate equations

One of the main aims of this work was to develop a model describing the fluorescence kinetics of CFP and YFP as single proteins as well as as parts of CFP–GBP–YFP. The detailed formalism and description of this model are given in the ESI†, here we outline its principal concepts.

Fig. 2 shows a schematic energy representation of the CFP–GBP–YFP construct. Both the donor and acceptor of the FRET protein are modelled as two-state systems. The first excited state of CFP lies at 2.7 eV. In YFP, it is situated at a slightly lower energy, 2.4 eV. These values were derived from our fluorescence measurements.

Various interactions of the fluorescent proteins of CFP–GBP–YFP with photons are also illustrated in Fig. 2. Both fluorescent proteins can absorb photons at the incident wavelength λ_{exc} and become excited to their higher energy states. The absorption process is described by a wavelength-dependent absorption cross section σ, which differs for the two proteins. The fluorescent proteins in excited states undergo spontaneous transition to the ground state with decay rates W_{CFP} and W_{YFP}. We prefer here the use of decay rates instead of their inverse, the decay times, because of their more intuitive description of the statistical nature of fluorescence

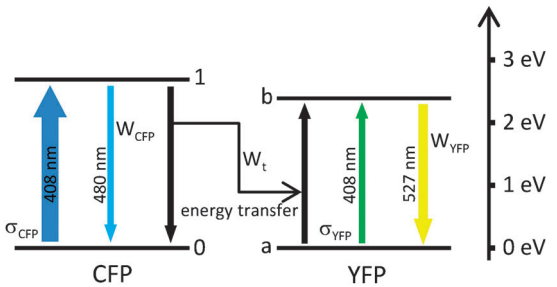

Fig. 2 Schematic of the rate equation model for the FRET pair CFP–YFP. The parameters that describe the individual processes are indicated in the figure. Fluorescence excitation in our experiments took place at 408 nm.

emission as well as the reduced complexity of equations accompanying their use. Please note that the spontaneous decay rates W_{CFP} and W_{YFP} are the sum of the respective radiative and non-radiative decay rates. The wavelengths associated with these transitions in CFP and YFP are indicated in Fig. 2.

The process of photon emission from either protein i is described by the radiative decay rates W_i^{rad}, which must be smaller or equal to the observed decay rate W_i. In addition, in CFP–GBP–YFP, energy can be transferred from CFP in its excited state to the ground state YFP. This is described by the transfer rate coefficient W_t. Due to the nature of the given FRET construct, the distance between CFP and YFP can only take specific values, corresponding to the closed *vs.* open state of the GBP moiety. The energy transfer rate thus only takes two distinct values.

In CFP–GBP–YFP, there is a fixed 1 : 1 relationship of the concentrations of CFP and YFP, and both correspond to the concentration of the construct. We will keep this relationship in mind, even though we use individual concentrations N_{CFP} and N_{YFP} when we formulate the model, as this allows a better understanding of processes and easier generalisation of the results to energy transfer processes between other FRET pairs and/or in different configurations (free, tethered). Furthermore, at the protein concentrations in our experiments, the closest YFP to any CFP is always the YFP linked to the CFP *via* GBP. Energy transfer from CFP is thus assumed to be exclusively intramolecular and to be accepted by YFP in the same protein. The consequence of this fact is that the energy transfer rate in our system depends exclusively on the conformation of GBP.

The models for the individual proteins CFP and YFP are special cases of the model for CFP–GBP–YFP, using the respective energy level structure, but setting the energy transfer rate $W_{tr} = W_t N_{YFP} = 0$ and considering only the energy levels of the protein of interest.

The model was applied in the following sections to describe the experimental data and to extract quantitative parameters characterizing the proteins' optical properties. These in turn can be used for predictive modelling of their photophysical behaviour in engineered assemblies, such as biosensors.

Results and discussion

We first quantitatively determined the parameters of the model described in the previous section and the ESI.† Then we report the behaviour of the fluorescence emitted by CFP–GBP–YFP when it changes conformation on interacting with Ca^{2+} and analyze the situation with the help of the model. At the end, we discuss its strengths and limitations.

Absorption cross sections

Uptake of an excitation photon is the first step in the cascade leading to the emission of fluorescence. It is described quantitatively by the absorption cross section σ. Fig. 3(a) shows the absorption cross sections of the individual proteins CFP and YFP and of the FRET construct CFP–GBP–YFP. The data were obtained from transmission measurements. Overall, two absorbing regions can be distinguished: the one between 375 nm and 475 nm is attributed to CFP, the other between

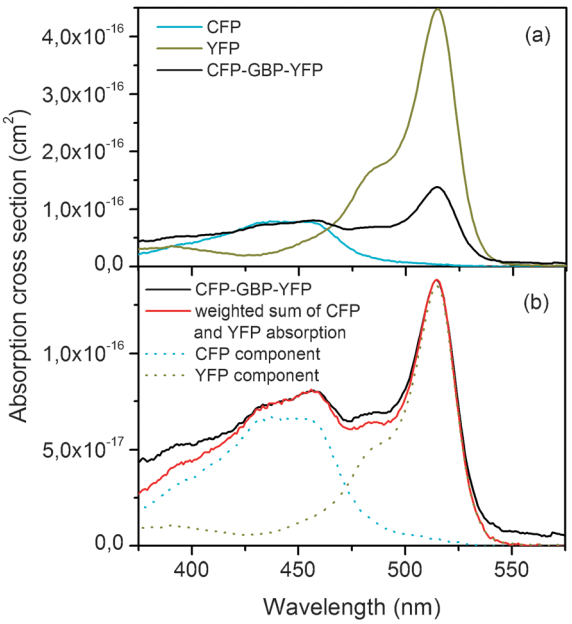

Fig. 3 (a) Absorption cross sections of CFP, YFP and CFP–GBP–YFP in phosphate saline. (b) Absorption cross section of CFP–GBP–YFP decomposed into its components due to CFP and YFP. The weighted sum of the individual components reproduces the absorption of the compound protein CFP–GBP–YFP very well, indicating that in the spectral range between 400 nm and 550 nm its absorption is completely determined by the fluorescent moieties CFP and YFP.

Table 1 Absorption cross sections at maximum absorption for CFP, YFP and the FRET construct CFP–GBP–YFP

Protein	λ_{max}/nm	σ_{abs}/cm^2
CFP	440	7.9×10^{-17}
YFP	515	4.5×10^{-16}
CFP–GBP–YFP	515	1.4×10^{-16}

450 nm and 550 nm to YFP (Table 1). CFP has its absorption maximum at 440 nm, YFP at 515 nm. The absorption of CFP–GBP–YFP also peaks at 515 nm due to the dominance of the YFP absorption component. However, compared to the absorption of free YFP, the absorption originating from the YFP component in CFP–GBP–YFP is reduced threefold. In contrast, the line strength of the CFP component is close to that of free CFP.

To assess possible spectral changes of the absorption cross section of CFP and YFP in CFP–GBP–YFP, its absorption line was reconstructed from CFP and YFP absorption data (Fig. 3(b)). A weighted sum of CFP and YFP absorption cross sections nicely reproduces the absorption cross section of CFP–GBP–YFP. Only in the region of short wavelengths up to 400 nm, an additional component is apparent. This may suggest small contributions from the GBP moiety. We conclude that over the complete visible range, the absorption of CFP–GBP–YFP is determined predominantly by the absorption of its CFP and YFP groups.

The weights for the CFP and YFP components giving the highest quality reconstruction amount to 0.85 for CFP and

0.30 for YFP. They were determined in terms of the absorption cross section of the free proteins and indicate deviations from free protein behaviour caused by their integration into CFP–GBP–YFP. While the deviation of CFP is minor, that of YFP is large and significant. We have measured similar deviations in other FRET constructs (unpublished results). This phenomenon, which to a lesser degree is also observed in mixtures of CFP and YFP, is most likely due to the specific molecular environment created by the attachment of YFP and CFP to GBP. The changed molecular environment after attachment to the functional group influences the properties of the electronic dipole responsible for light absorption. This result, together with structural information on the proteins, may provide deeper insights into the mechanisms of optical absorption of the fluorescent proteins.

An alternative interpretation, namely a lower than stoichiometric attachment of active YFP to CFP–GBP–YFP, is excluded because CFP–GBP–YFP is produced as a single polypeptide. Moreover, in CFP–YFP mixtures a less pronounced, but noticeable decrease of the absorption line strengths is observed.

The above result is very important for any quantitative evaluation of fluorescence from a FRET protein, *e.g.* in spectroscopy or biosensors. It indicates that from a measurement of the free protein absorption cross section it is not possible to infer quantitatively the absorption properties of a FRET construct consisting of the same fluorescent proteins.

Of particular interest is the absorption cross section of CFP and YFP in CFP–GBP–YFP at the excitation wavelength. There, absorption is dominated by the CFP component while that of YFP cannot be determined. However, reconstruction of the CFP–GBP–YFP absorption cross section from CFP and YFP cross sections allows determination of the absorption cross sections of the CFP and YFP moieties in CFP–GBP–YFP (Table 2). The strong decrease in YFP absorption line strength after attachment to GBP reduces direct absorption by YFP and thus helps to create a FRET protein where energy transfer dominates the direct excitation of the acceptor even more than expected from the properties of the free donor and acceptor proteins.

Fluorescence emission

Fluorescence was excited at 405 nm. At this wavelength, CFP absorbs efficiently (absorption cross section of 3.9×10^{-17} cm^2), while the direct excitation of YFP is inefficient (absorption cross section of 1.1×10^{-18} cm^2; both values are given for CFP–GBP–YFP). The wavelength was chosen to allow study of energy transfer between CFP and YFP with the least possible direct excitation of YFP while maintaining high

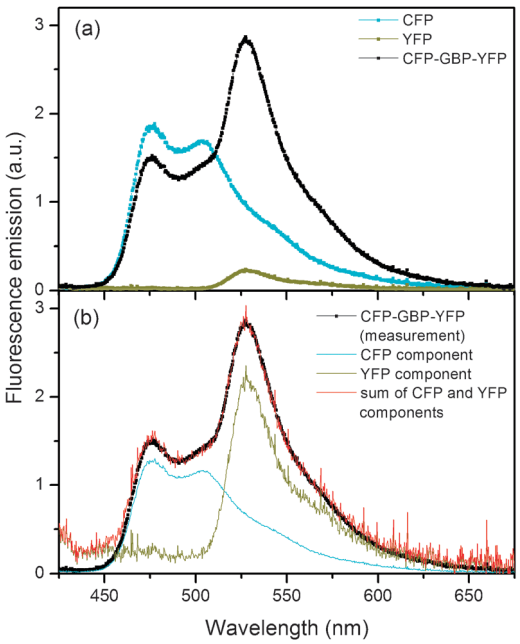

Fig. 4 (a) Fluorescence spectra of CFP, YFP, and CFP–GBP–YFP under excitation at 405 nm. High emission from CFP and low emission from YFP demonstrate the suitability of this excitation regime for the FRET pair CFP–YFP. (b) The fluorescence spectrum of CFP–GBP–YFP can be reproduced by the weighted sum of CFP and YFP fluorescence spectra. No additional fluorescence components are present in the spectrum. The high noise level in the reproduction is due to the high weight factor for the YFP spectrum.

CFP excitation efficiency. As shown in Fig. 4(a), CFP emits in the 450–600 nm spectral range, with its fluorescence peak at 478 nm, YFP in the range from 500 nm to 600 nm, with its maximum at 527 nm. The fluorescence emission from free YFP is considerably lower than that of CFP, due to its one order of magnitude smaller absorption cross section at the excitation wavelength.

The fluorescence from CFP–GBP–YFP shows distinct signs of the emission lines from both CFP and YFP: its emission maximum is at 527 nm similarly to that of YFP, and the shoulder between 450 nm and 500 nm has a spectral shape identical to that of the emission from CFP. To extract CFP and YFP components from the fluorescence of CFP–GBP–YFP, we again used a reconstruction method: a weighted sum of CFP and YFP fluorescence perfectly reproduces the CFP–GBP–YFP fluorescence (Fig. 4(b)). No additional (auto)fluorescence component arises from GBP in this spectral range under excitation at 405 nm. The weights of the CFP and YFP components with respect to the emission of the free proteins amount to 0.69 and 9.5, respectively. Considering the

Table 2 Summary of the parameters of the model presented in Results and discussion as derived from measurements reported in this article. The subscripts CFP and YFP indicate the free proteins, while FRET signifies properties of the CFP–GBP–YFP FRET construct. Note that the decay rates for CFP were determined as aggregate decay rates over the double exponential decay

Parameter	Value	Parameter	Value
σ_{CFP} (405 nm)	4.6×10^{-17} cm^2	W_{CFP} (aggregate)	3.3×10^{8} s^{-1}
σ_{YFP} (405 nm)	3.5×10^{-18} cm^2	W_{CFP} (FRET, aggregate)	5.0×10^{8} s^{-1}
$\sigma_{FRET/CFP}$ (405 nm)	3.9×10^{-17} cm^2	W_{YFP}	2.9×10^{8} s^{-1}
$\sigma_{FRET/YFP}$ (405 nm)	1.1×10^{-18} cm^2	W_{tr} (aggregate)	1.7×10^{8} s^{-1}

differences in the absorption cross section and assuming that the radiative decay rate of fluorescence from CFP and YFP attached to GBP is identical to that of the free proteins, we conclude that the emission of CFP is reduced by 20% and that of YFP is increased by a factor of 32. These effects are attributed to energy transfer from CFP to YFP. Energy absorbed by CFP and transferred to YFP is no longer available for emission by CFP, thus resulting in a decrease of CFP fluorescence. Furthermore, the large increase of emission intensity from YFP in CFP–GBP–YFP demonstrates the suitability of the excitation regime for measurement of FRET with only little interference from fluorescence excited *via* direct absorption by YFP.

Fig. 4(b) also plots the CFP and YFP components of the reconstruction separately. A significant fraction of CFP fluorescence is present at the position of the emission maximum from YFP. The fluorescence intensity there, *i.e.* at 527 nm, is therefore determined by the fluorescence emitted from both CFP and YFP. This must be taken into account when a quantification of the YFP emission from the FRET construct is required. The reconstruction method provides a safe way for such an evaluation and helps to avoid mistakes due to overlapping emission lines in a FRET spectrum.

Fluorescence excitation

To corroborate the FRET results obtained from steady state emission measurements, we performed fluorescence excitation spectroscopy on CFP–GBP–YFP. These are depicted in Fig. 5, together with absorption data taken from Fig. 3. Fluorescence at 476 nm was monitored to obtain the excitation spectrum of CFP in the FRET construct, and YFP emission was characterised by fluorescence at 527 nm. Please note that the fluorescence at 527 nm does not purely originate from YFP, but contains a component of the CFP fluorescence, as outlined above.

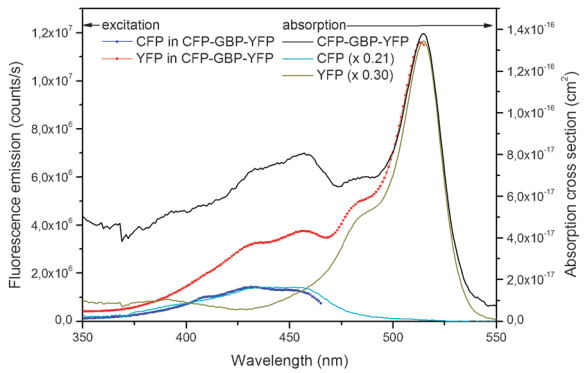

Fig. 5 Comparison of excitation spectra for the CFP and YFP components of the CFP–GBP–YFP FRET protein with the absorption cross sections of CFP and YFP. CFP and YFP emission were monitored at 476 nm and 527 nm, respectively, while the excitation wavelength was scanned over the range indicated on the *abscissa*. The absorption data were taken from Fig. 3. The excitation of CFP fluorescence in the CFP–GBP–YFP construct follows the CFP absorption closely. In contrast, YFP fluorescence can be excited not only in the range of YFP absorption, but also in the range of CFP absorption. This indicates the presence of energy transfer from CFP to YFP.

CFP fluorescence from CFP–GBP–YFP can be excited in the range from 375 nm up to the monitoring wavelength of 476 nm, as shown in the figure, in spectral agreement with the absorption line of free CFP. In contrast, emission of the YFP component of CFP–GBP–YFP can be excited even at wavelengths where free YFP does not absorb significantly. Excitation of the YFP component of the FRET protein is possible starting from 375 nm up to the monitoring wavelength at 527 nm. While the excitation spectrum of the YFP fluorescence component is very similar to the absorption spectrum of free YFP between 475 nm and 550 nm, it bears a strong resemblance to the absorption spectrum of free CFP between 375 nm and 475 nm. This again is an indication that energy transfer from CFP is the dominant mechanism of excitation of YFP at wavelengths shorter than 475 nm. Indeed, the excitation spectrum for the YFP component is well reproduced by a linear combination of the absorption cross sections of free CFP and YFP (not shown).

The excitation spectrum of the YFP component does not exclusively follow the absorption line shape of the CFP–GBP–YFP FRET construct. If both are normalised to their maxima, clear deviations appear in the wavelength range where CFP absorbs. This phenomenon is apparent in Fig. 5. The reason for this is two-fold: first, as described in the discussion of Fig. 3, the absorption line at short wavelengths contains an apparent contribution which may be associated with the presence of GBP. This absorption does not contribute to the excitation of either the CFP or YFP moieties in the FRET protein. However, it increases the absorption cross section in that wavelength range. Second, a match between absorption and excitation of the acceptor fluorescence of a FRET construct is only expected in the case where the energy transfer efficiency between a donor (CFP) and an acceptor (YFP) is unity. This corresponds to an infinite energy transfer rate W_{tr}. In that case, the donor does not emit fluorescence. The fact that we measure CFP fluorescence from CFP–GBP–YFP thus can be traced to the same origin as the deviation in the line shape between absorption of CFP–GBP–YFP and excitation of its YFP moiety, namely an energy transfer efficiency of less than one.

Fluorescence decay kinetics

A clearer picture of the energy transfer is afforded by direct measurement of the fluorescence decays of free CFP and YFP and CFP–GBP–YFP. In contrast to steady-state spectroscopy, it allows easy quantification of the energy transfer rate. The fluorescence decay measurements were obtained by spectrally-resolved time-correlated single photon counting.

Fig. 6(a) shows the fluorescence decays of CFP as free protein and as part of CFP–GBP–YFP. The traces were measured at 488 nm. The decay trace at this wavelength is representative of CFP fluorescence kinetics over the whole CFP wavelength range, no significant differences at other wavelengths were observed (see Fig. 7). The data for free CFP can be fitted well with a double-exponential function $I(t) = a_1 \exp\{-W_1 t\} + a_2 \exp\{-W_2 t\}$ with adjustable parameters a_1, a_2, W_1, W_2. a_1, a_2 are the weights of the two exponential components and W_1, W_2 their decay rates according to the definitions in the model, *i.e.* the inverse of the fluorescence

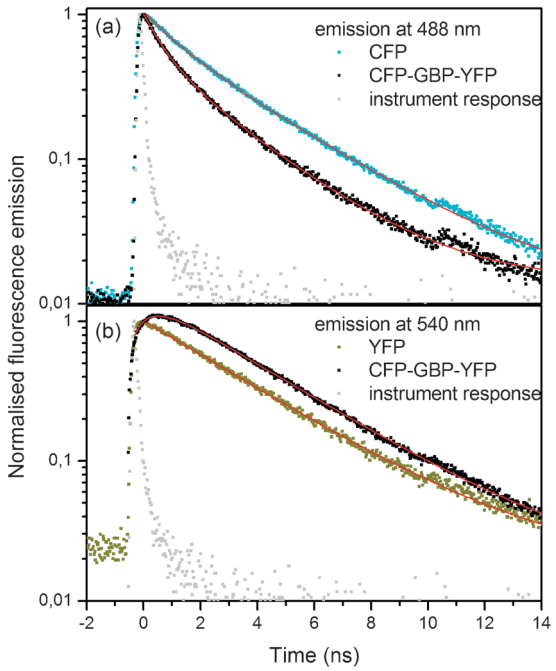

Fig. 6 Comparison of the fluorescence decays of CFP and YFP in CFP–GBP–YFP to those of the free fluorescent proteins CFP and YFP: (a) CFP component, evaluated at an emission wavelength of 488 nm. (b) YFP component, evaluated at an emission wavelength of 540 nm. The component in the decay measured at 540 nm of CFP–GBP–YFP due to the long wavelength tail of CFP emission was removed by subtraction, the data therefore represent only the decay of the YFP component. The deviations between the two decay traces in both parts of the figure are due to energy transfer between CFP and YFP. Exponential fits to the data are shown as red lines, the instrument response as grey squares.

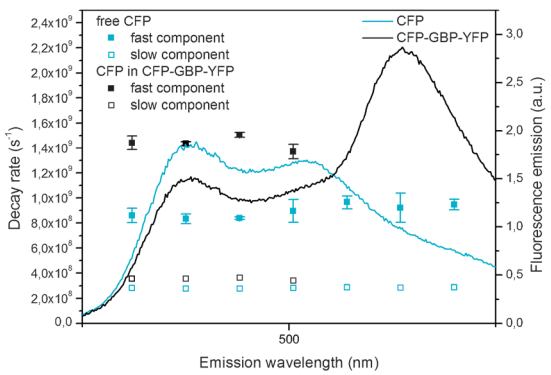

Fig. 7 Fast and slow decay rates of CFP as a function of wavelength. Both for free CFP and for CFP as part of the FRET protein CFP–GBP–YFP, the decay rates are independent of wavelength within the experimental error. In the case of CFP in CFP–GBP–YFP, the data extend only over the wavelengths whose emission can unambiguously be attributed to CFP. For free CFP, data across the whole fluorescence spectrum are shown. Data points are means with standard deviations over four measurements. The error bars on the slow decay components are negligible compared to the size of the symbol and for reasons of clarity are omitted.

decay times. The fast decay rate W_1 as evaluated from the data in Fig. 6(a) amounts to $8.3 \times 10^8 \pm 3.2 \times 10^7\ s^{-1}$ with a weight of 0.32, the slow decay rate W_2 takes the value of $2.8 \times 10^8 \pm 4.7 \times 10^6\ s^{-1}$ and has a weight of 0.68. The errors on decay rates given here and in the following were derived from the quality of the fit. These decay rates are in excellent agreement with the data reported for ECFP in aqueous solution by Borst *et al.*[30] ($W_1 = 8.8 \times 10^8\ s^{-1}$, $W_2 = 2.7 \times 10^8\ s^{-1}$, $a_1 = 0.335$ and $a_2 = 0.665$), Jose *et al.*[31] ($W_1 = 8.9 \times 10^8\ s^{-1}$, $W_2 = 3.07 \times 10^8\ s^{-1}$, $a_1 = 0.4$ and $a_2 = 0.6$ at pH 7.5), and similar to data from CFP-transfected cells by Tramier *et al.*[32] ($W_1 = 7.7 \times 10^8\ s^{-1}$, $W_2 = 2.6 \times 10^8\ s^{-1}$, $a_1 = 0.53$ and $a_2 = 0.47$). The weights reported for the cellular environment differ somewhat from our measurements, which may be an indication for a dependence of the CFP conformation equilibrium on its environment or on the route of synthesis.

Fig. 6(a) shows clearly how the fluorescence decay of CFP changes when it is introduced into CFP–GBP–YFP. Its fast decay rate nearly doubles to $1.5 \times 10^9 \pm 3.0 \times 10^7\ s^{-1}$ and increases in weight to 0.44. The slow decay rate increases moderately to $3.7 \times 10^8 \pm 3.7 \times 10^6\ s^{-1}$.

Under the assumption that all decay rates of CFP are independent of the protein's environment (and whether it is bound to GBP or not), a presumption that is at least rudimentarily backed by the similarity of the decay rates evaluated in the cellular environment[32] to ours in buffer solution, we can estimate the energy transfer rate W_{tr} according to eqn (S5) in the ESI.† However, the double-exponential decay of CFP requires some consideration before applying the equation. A double exponential fluorescence decay is possible in only two cases: (a) there exist two distinct protein conformations, such as those reported for CFP,[33] between which no energy migration takes place, neither between their excited nor their ground states; or (b) the two decay rates can be due to different reaction kinetics from two distinct molecular conformations into an identical excited state,[34] although this should in fact give rise to a triple exponential decay. Again, no energy migration may take place between the two conformations.

Both possibilities have been discussed. In either case, the pre-exponential factors in the CFP decay reflect the percentage of molecules in the two distinct conformational states. As neither the decay rates of CFP show any dependence on emission wavelength, nor the emission spectrum on excitation wavelength, it must be concluded that the energy levels of the two conformations are identical. Thus the two types of physical processes cannot be distinguished based on kinetic and steady-state optical data. It also means that both conformations interact with and transfer energy to YFP. Therefore, we will retain the formulation of our model with a single decay rate for its simplicity, and apply it separately for the two decay rates of CFP. However, given the evidence that the two conformations of CFP do not interact with each other, a complete model over the ensemble can be created by summing over the contributions of the individual conformations.

The fluorescence intensity of all proteins as a function of their concentration is linear up to concentrations of $\sim$20 μM, indicating the onset of energy migration between proteins of the same species only at concentrations an order of magnitude higher than used for the measurements reported here. Thus, from a molecular perspective, it seems adequate and useful to determine separate energy transfer rates for CFP with fast and slow decays, in light of the interpretation of the two decay

rates as a signature of two distinct conformational states. These can be calculated as the difference between the respective decay rate of CFP in the FRET protein and that of its free counterpart. They amount to 6.7×10^8 s^{-1} for the fast decay and 9.0×10^7 s^{-1} for the slow decay. The energy transfer efficiency $\eta_{tr} = W_{tr}/(W_{tr} + W_{CFP})$ amounts to 0.45 and 0.24 for the two types of CFP conformations, respectively. This means that nearly half of the energy absorbed by CFP with fast decay is transferred to YFP. For CFP with slow decay it is only close to a quarter.

While the differentiation between two decay and energy transfer rates is of preference in view of a molecular understanding of the optical processes in FRET proteins, for the sake of clarity and ease of comparison we define an aggregate decay rate for an arbitrary decay function as

$$W_i = \frac{\Phi_i^{max}}{\int_0^\infty \Phi_i dt} \quad (1)$$

Here the index i identifies the fluorescing species. Φ is the fluorescence photon flux, its initial value in the decay trace is denominated Φ^{max}. This definition of the decay rate equates the integral under the fluorescence decay curve with that of a single exponential function and assigns the exponential constant as an equivalent decay rate. It corresponds to a weighted average of the contributing decay rates. The aggregate value according to the above definition amounts to 3.3×10^8 s^{-1} for free CFP and 5.0×10^8 s^{-1} for CFP as part of the FRET construct, giving an aggregate energy transfer rate of 1.7×10^8 s^{-1}. This definition unfortunately ignores differences in the pre-exponential factors of the CFP decay in the free and FRET proteins, and should thus be used only indicatively.

Moving from CFP to YFP fluorescence decay, Fig. 6(b) shows the corresponding decay traces for YFP as a free protein and as part of the CFP-GBP-YFP construct. The measurements shown in the figure were obtained at a wavelength of 540 nm. The decay of free YFP is very close to single exponential with a decay rate of $2.9 \times 10^8 \pm 1.2 \times 10^6$ s^{-1}. Determination of the YFP decay rate in the FRET construct is somewhat more difficult because, as emphasised above, the decay trace at 540 nm contains contributions from both YFP and CFP (*cf.* Fig. 4(b)). Therefore, from the measured decay trace at 540 nm, we need to subtract the contribution from CFP emission to extract the fluorescence decay originating from YFP.

As we have seen, the decay rates of CFP in CFP–GBP–YFP are different from those of free CFP. Thus we cannot *a priori* use the decay traces of free CFP for such a correction. The correction can, however, be achieved in the following manner, which is similar to spectral unmixing: as demonstrated in Fig. 4(b), the spectral shapes of CFP as a free protein and CFP in CFP–GBP–YFP are identical. We can therefore use the spectrum of free CFP to determine the total intensity ratio of the CFP component in the FRET construct at 488 nm and 540 nm. Combining this intensity information with the characteristic shape of the decay trace of the CFP moiety in CFP–GBP–YFP (measured at 488 nm), we generate a decay trace with the actual decay constants of CFP in the FRET construct, whose intensity corresponds to that of CFP at 540 nm. This treatment is valid, as long as the decay rate of CFP (free or as part of CFP–GBP–YFP) is constant over its spectrum. Fig. 7 shows the measured decay rates as a function of the emission wavelength. Within the precision of our measurement, the decay rates are constant over the whole wavelength range of CFP emission. The same holds true over the whole wavelength range where fluorescence can be unambiguously attributed to CFP in CFP–GBP–YFP. The above assumption is therefore justified. Please note that this finding contradicts the recent results by Villoing *et al.*,[28] who found an increase in the decay rate of ECFP with increasing emission wavelength but do not report on its origin.

As a result of the above correction procedure, after subtraction of the CFP-related decay at 540 nm from the measured decay trace of the FRET construct, we obtain the true decay trace of YFP in CFP–GBP–YFP. This decay trace is the one shown in Fig. 6(b).

The decay from YFP in CFP–GBP–YFP shows a pronounced concave curvature at short times and approaches the decay trace of free YFP for long times. This feature is caused by feeding of energy into the YFP excited state from CFP and is well described by eqn (S5) in the ESI.† Fitting a double exponential function, one of whose pre-exponential coefficients is negative, to the trace, we obtain the rate associated with the decay of YFP as $2.9 \times 10^8 \pm 1.4 \times 10^6$ s^{-1}, in perfect agreement with the decay rate for free YFP. The rate associated with the feeding of energy into the YFP excited state amounts to $1.6 \times 10^9 \pm 4.5 \times 10^7$ s^{-1}, which corresponds within the margin of error to the fast decay rate of CFP in the FRET protein—exactly as predicted by eqn (S5) (ESI†).

A similar feeding effect as seen for the energy transfer involving CFP with fast fluorescence decay is expected for the one with slow fluorescence decay. The feed rate must amount to 3.7×10^8 s^{-1} according to eqn (S5) (ESI†), the decay rate measured for the slow fluorescence decay of CFP as part of the FRET protein. However, it was not possible to extract this value from the data given in Fig. 6(b) in a conclusive manner: although the decay trace can be fitted with a triple exponential involving contributions with the fast and slow decay rates of CFP as feeding mechanism and decaying with the decay rate of YFP, the quality of the fit does not increase over the double exponential one described above. The feed rate caused by energy transfer from CFP with slow fluorescence decay apparently lies too close to the spontaneous YFP decay rate to allow its discrimination. However, its presence cannot be excluded. Nonetheless, from the energy transfer rates and evidence of the feeding term in the decay trace of YFP, we can conclude that the two CFP conformations transfer energy with different rates to YFP and that CFP with fast fluorescence decay is the dominant donor in the energy transfer to YFP (Table 2). Together with the absorption cross sections (given at 405 nm), the decay rates of the CFP and YFP components of the CFP–GBP–YFP determine the excitation density in the excited states of the fluorescent proteins as a function of the photon flux of radiation at the excitation wavelength and the protein concentration. We have shown that the spontaneous decay rate of YFP is independent of whether it is attached to GBP or not. We have calculated

energy transfer rates between CFP and YFP in CFP–GBP–YFP under the assumption that this is true also for CFP. In order to complete the optical model and allow calculation of fluorescence photon emission densities in a system containing CFP–GBP–YFP FRET proteins (*cf.* eqn (S10) in the ESI†), the radiative decay rates of CFP and YFP must be determined. This can be done with the help of the measured decay rates in conjunction with the quantum efficiencies for CFP and YFP determined experimentally by Patterson *et al.*[35] With fluorescence quantum efficiencies of 0.4 for CFP (in good agreement with our own measurements not reported here) and 0.6 for YFP, the radiative decay rates of CFP and YFP amount to 1.3×10^8 s^{-1} and 1.7×10^8 s^{-1}, respectively.[36]

The full set of parameters characterising CFP, YFP and CFP–GBP–YFP according to the model is summarised in Table 2.

Effects of changes in protein conformation

GBP has a binding site for Ca^{2+} that is structurally similar to the Ca^{2+}-binding element in the well-known EF-hand class of proteins, but comes in two halves (residues 157–165 and 227–228).[37] Ca^{2+} binding enhances the thermal stability of GBP.[38,39]

In this section, we will show that FRET can be used to monitor binding and release of Ca^{2+} and the resulting change in the conformation of GBP. Conformational changes in GBP cause the distance between CFP and YFP to vary and lead to concomitant variations in FRET efficiency. In principle, FRET efficiency provides a scale for the distance between CFP and YFP, under the assumption of dipole–dipole energy transfer,[16] and knowledge of the Förster radius. However, independent of the determination of distances, monitoring the energy transfer efficiency between donor and acceptor moieties of a FRET protein provides a route to visualise the reaction of protein conformation to the presence or absence of specific ions or molecules. In addition, use of proteinaceous fluorophores entails the possibility that the fluorophores themselves may display optical alterations that result from conformational changes rather than a mere change in the physical distance between the fluorophores.

Fig. 8 compares the fluorescence emission spectrum from CFP–GBP–YFP with an occupied Ca^{2+}-binding site with that of one with an empty binding site. The latter was obtained by adding 2 mM EDTA to the solution containing CFP–GBP–YFP and incubating over night. An unoccupied binding site leads to an increase in the fluorescence emission from CFP and a decrease in the emission from YFP, as is evidenced by the increase of the shoulder of the fluorescence spectrum at 470 nm and a decrease of the peak at 527 nm.

The increase in CFP emission and the concomitant decrease of YFP emission suggest a reduction of the energy transfer efficiency between the two fluorescent moieties of CFP–GBP–YFP when Ca^{2+} is removed from its binding site. All other parameters being constant, this can only be caused by an increase in the distance between CFP and YFP as a consequence of a conformational change of the central GBP protein upon Ca^{2+} release. The conformational change is

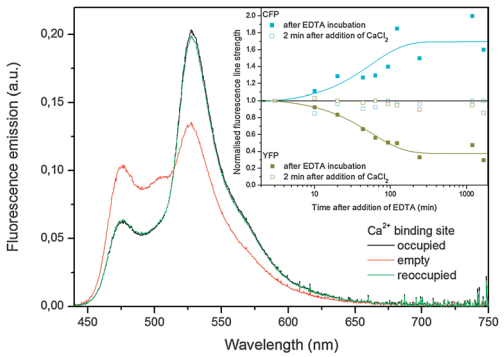

Fig. 8 Fluorescence emission from CFP–GBP–YFP with occupied and unoccupied binding sites for Ca^{2+}. Ca^{2+} release is achieved by chelation with EDTA and leads to a loss of FRET, indicating a conformational change of the protein. FRET is recovered on reoccupation of the binding site with Ca^{2+}. The inset shows the normalised fluorescence line strengths of CFP and YFP for EDTA incubations of different durations. This allows tracing the release reaction of Ca^{2+} due to competition between the FRET protein and EDTA in the sample as a function of time. A time constant of approximately 55 min is extracted assuming an exponential time dependency.

reversible (Fig. 8): upon addition of 5 mM $CaCl_2$ to CFP–GBP–YFP, the original shape of the spectrum with dominating YFP emission is recovered. This indicates that the CFP and YFP moieties move to their original, more proximal positions when GBP changes its conformation again to accommodate Ca^{2+}.

The inset to Fig. 8 compiles the results of a series of such experiments. Several samples with an identical composition were prepared, providing originally a Ca^{2+}-rich environment for CFP–GBP–YFP. After an initial recording of the fluorescence spectrum, 2 mM EDTA was added to chelate away Ca^{2+}. After a specific time of incubation in the solution containing EDTA, a second spectrum was recorded. This incubation time is represented on the *abscissa* of the inset. Immediately after the second spectrum was measured, 5 mM $CaCl_2$ was added to the solution. After a two minute reaction time to reach equilibrium, a third spectrum was recorded as evidence of the recovery of the original FRET efficiency and to exclude the possibility of non-reversible effects.

All resulting spectra were decomposed into their CFP and YFP components by the method described earlier. The second and third recordings were normalised to the values of the respective initial measurement to eliminate the influence of potential concentration errors. The inset to Fig. 8 shows the normalised values of the CFP and YFP components of the fluorescence spectrum after incubation with EDTA as solid squares, and the respective measurements after addition of $CaCl_2$ as open squares.

Increasing incubation time with EDTA causes a gradual increase in the fluorescence signal attributed to CFP and a corresponding decrease of the fluorescence signal from YFP. Independent of the incubation time with EDTA, the original signal can be recovered completely by addition of $CaCl_2$. The binding/release reaction of Ca^{2+} with GBP in the FRET construct thus appears to be completely reversible. The drawn lines in the inset are exponential fits to the data obtained after incubation with EDTA. The exponential time constant of the

fit amounts to 55 min and gives an indicative value for the time constant of the competitive reaction between Ca^{2+} and the FRET construct and 2 mM EDTA, respectively.

In this context, recall that each single CFP–GBP–YFP is presumed to take only two distinct FRET states, associated with occupied and unoccupied Ca^{2+} binding sites. The gradual change of the fluorescence spectrum seen in the inset of Fig. 8 originates from a change in the fraction of CFP–GBP–YFP with an occupied Ca^{2+} binding site. The measurements at each point in time represent ensemble averages over CFP–GBP–YFP with a certain fraction of occupied and unoccupied Ca^{2+} binding sites.

Fig. 9 shows normalised fluorescence decay traces of CFP–GBP–YFP at 488 nm and 540 nm for various incubation times. The traces of CFP–GBP–YFP measured at 540 nm had the CFP component at that wavelength subtracted in the manner described above, therefore they are representative of the decay of the YFP component. In addition to the fluorescence decays of the FRET protein, the decay traces of free CFP at 488 nm and free YFP at 540 nm are added to the figure for comparison.

Fig. 9(a) shows that the CFP decay decelerates with increasing incubation time in EDTA. For long incubation times, the decay trace approaches, but does not completely reach, the fluorescence decay of free CFP. This can be explained by analogy to the behaviour of the steady-state fluorescence from the FRET construct (see Fig. 8 and the corresponding discussion).

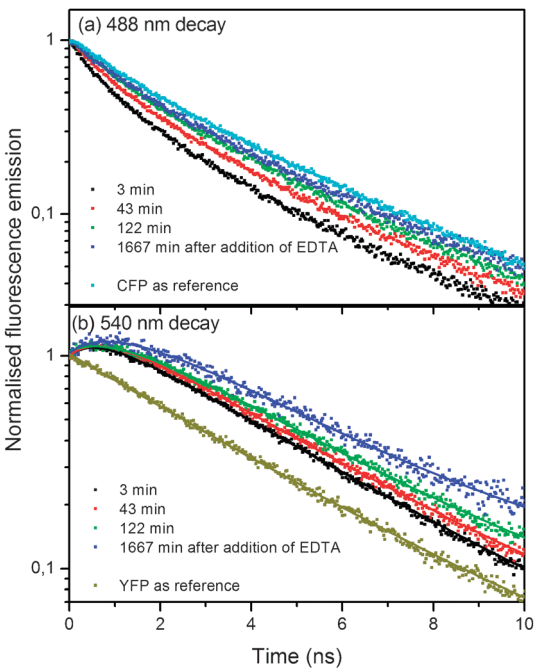

Fig. 9 Fluorescence decay traces of (a) the CFP and (b) the YFP component of the FRET construct CFP–GBP–YFP as a function of the incubation time with EDTA. The traces in (b) were corrected for the fluorescence tail of CFP and represent the fluorescence originating from YFP only. Double exponential fit curves according to eqn (S5) (ESI†) were added in (b) to illustrate the feeding mechanism of energy into YFP. The reduction of FRET with increasing incubation time is clear from a consecutively slower fluorescence decay of CFP and correspondingly slower feeding of energy into YFP.

The more Ca^{2+} is removed from its binding site on GBP, the slower are the apparent decay rates of CFP. According to eqn (S5) in the ESI†, the measured decay rate consists of the sum of the spontaneous decay rate of CFP and the rate of energy transfer from CFP to YFP. It follows that removal of Ca^{2+} is associated with a decrease in the energy transfer rate and efficiency. This indicates that, by observing energy transfer, we indeed monitor a conformational change of CFP–GBP–YFP as a result of its binding or release of Ca^{2+}. During binding, GBP changes its conformation in such a way that the two fluorescent proteins are moved into close proximity. On release, the conformational change of GBP swings the two fluorescent proteins apart and thus reduces the efficiency of energy transfer between them. The energy transfer efficiency in the ligand-free apoprotein state, however, does not reach zero, as the fluorescent proteins are linked *via* the central protein. The distance between them cannot increase indefinitely. Thus energy transfer between CFP and YFP of a certain extent remains present even in the state where Ca^{2+} is not bound to GBP and the two fluorescent proteins are as far apart as possible in the given molecular system.

The numerical values for the fast and slow decay rates of CFP during the release of Ca^{2+} can be retrieved from Fig. 10. Both decay components behave in a similar way: their values are reduced with increasing incubation time and at long times approach values slightly higher than the corresponding decay rates of free CFP.

At this stage it is expedient to insert a brief aside. Above, we had calculated the energy transfer rate between CFP and YFP under the assumption that the spontaneous decay rates of CFP do not change when it is fused to GBP. The results of Fig. 9 indicate clearly that this assumption is close to reality. Although we cannot quantify the remaining effect of energy transfer between CFP and YFP after release of Ca^{2+} from GBP, the fact that the corresponding decay rates of CFP are coming very close to those of free CFP gives strong evidence that the attachment of CFP to GBP has little to no influence on the fluorescence decay rates of CFP.

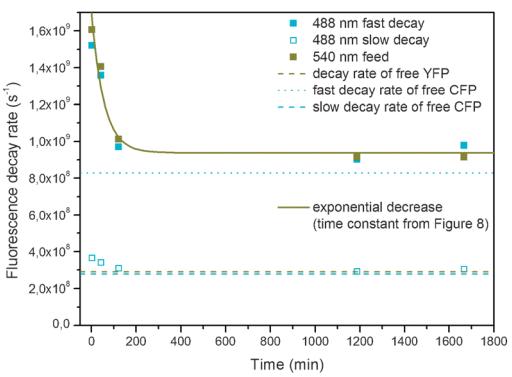

Fig. 10 Fluorescence decay rates of the CFP and YFP components in CFP–GBP–YFP as a function of the incubation time with EDTA. The fast decay rate of the CFP moiety corresponds excellently with the energy feeding rate into the YFP moiety. The solid line represents an exponential function with the same time constant as in the inset of Fig. 8. Broken lines indicate the values of the decay rates from free proteins CFP and YFP.

As discussed above, energy transfer between CFP and YFP is visible not only in the donor (CFP) decay but also in that of the acceptor, in this case YFP. This is depicted in Fig. 9(b). The decay traces of YFP in the FRET protein are concave up to a time of about 2 ns. This feature is associated with a feeding of energy into YFP from the CFP donor moiety and was already discussed above. The figure suggests that energy transfer persists even after long times of incubation with EDTA, *i.e.* when the fluorescent moieties of the FRET protein have reached their maximum distance from each other. However, with increasing distance, the mechanism transferring energy to YFP decreases in efficiency. Note that the same result was obtained from observation of the CFP fluorescence decay. Included in Fig. 9(b) are numerical fits of eqn (S5) (ESI†) to the decay traces. The fit quality is excellent. With the help of these numerical adjustments, the feed rate of energy into the YFP moiety of the FRET protein can be extracted. The corresponding rates are plotted together with the CFP decay rates in Fig. 10. The observed similarity of the YFP feed rate and the fast CFP decay rate as a function of the incubation time is striking and strongly supports the assumption that they originate from the same physical process, in line with our model eqn (S5) (ESI†). Note that, as discussed above, the slow CFP decay should lead to a corresponding slow feed rate into YFP. Unfortunately, the similarity of the slow CFP decay rate and the YFP decay rate prevents the extraction of the slow feed rate from our data.

Fig. 10 attempts to quantify the energy transfer between CFP and YFP in CFP–GBP–YFP as a function of the number of occupied Ca^{2+} binding sites (and their change in time during the reaction) by means of the decay rates. A similar quantification is shown in the inset of Fig. 8 based on the steady state emission intensities. These two independent approaches can be linked using the time dependency of the Ca^{2+} release reaction induced by competition of the FRET protein with EDTA. It was determined from the data in Fig. 8 as 55 min, assuming exponential behaviour. A function with an identical time constant is plotted in Fig. 10 and excellently describes the behaviour of the fast decay rate of CFP and the feed rate into YFP. Note that the corresponding line is fitted to the data in Fig. 10 using the time constant obtained from the data in the inset of Fig. 8. Thus, information obtained from steady-state intensity measurements and from decay rate measurements regarding the energy transfer between CFP and YFP in CFP–GBP–YFP are identical and may be used complementarily or alternatively in the qualification of conformational changes in such proteins.

Beyond the observation of temporal developments in the conformation of proteins, measurement of energy transfer in principle provides information on distance changes associated with conformational changes in CFP–GBP–YFP. Assuming Förster energy transfer, the relationship between donor–acceptor distance r and the efficiency of energy transfer η_{tr} can be written as

$$r = \sqrt[6]{R_0^6 \frac{1-\eta_{tr}}{\eta_{tr}}} \qquad (2)$$

R_0 is the Förster radius, which is defined as the distance between the donor and the acceptor where the energy transfer efficiency is 0.5. R_0 for the FRET pair eCFP/eYFP was determined by Patterson *et al.*[40] as 4.9 nm. Note that in that article R_0 was calculated from absorption and emission spectra and not measured in direct fluorescence experiments. We also recall that the energy transfer efficiency can be written in terms of decay rates as

$$\eta_{tr} = \frac{W_{tr}}{W_{CFP} + W_{tr}} \qquad (3)$$

When attempting to measure the distance between CFP and YFP in CFP–GBP–YFP, the non-single exponential decay of CFP forces us to make a choice regarding the definition for η_{tr} to use in eqn (2): either the energy transfer efficiency can be calculated for the fast and slow decay separately, or an aggregate transfer rate like the one given in eqn (1) can be employed.

From our data, we derive aggregate energy transfer efficiencies of 0.25 when the Ca^{2+} binding site of GBP is occupied and the fluorescent proteins are close together, and 0.05 after Ca^{2+} release when the fluorescent proteins reach their apparent maximum distance. These values, according to eqn (2), translate into distances between the active sites of CFP and YFP of 5.9 nm and 8.0 nm, respectively. If the fast and slow decay rates of CFP are used instead, distances between 5.0 nm and 7.4 nm are obtained. It is, however, unclear whether the Förster radius determined for the aggregate system from absorption and emission spectra[40] is applicable when using the two rates determined from the fluorescence decay. Rather, assuming the distance between CFP and YFP to depend only on the conformation of GBP, it is likely that the different energy transfer efficiencies for the two decays are associated with respective Förster radii for the two CFP conformations.

In order to turn the detection of conformational changes *via* FRET into a quantitative technique, two issues need to be considered: first, we need to achieve coupling between the distances determined optically and the structural properties of the protein. This would require high resolution measurement of the maximum diameter of the CFP–GBP–YFP protein in the presence and absence of Ca^{2+}. We are exploring two methodological approaches in this direction: the use of quasi-elastic laser light scattering and ion mobility spectroscopy. Combined preliminary data have yielded measurements of the diameter of the ligand-free apoprotein particle in the range of 9.2–9.5 nm, suggesting that the Förster radius determined above would be contained within the physical boundaries of the protein.

Second, the above mentioned ambiguity as to the choice of energy transfer rates in the determination of the distance between the fluorescent proteins needs to be resolved. This choice is relevant for all FRET couples whose donor has a multiexponential fluorescence decay, not only for CFP–YFP. In the case discussed above, a distance evaluation using the individual slow or fast decay rates or an aggregate decay rate leads to three different sets of distances between the fluorescent proteins in the open and closed states. It is obvious that currently this technique cannot be used to measure absolute distances unless a clear understanding of the processes

underlying the double exponential decay in CFP is developed. Further work needs to be performed to understand the electronic mechanism behind the non-single exponential fluorescence decay of CFP, or recourse needs to be taken to variants of CFP with single exponential fluorescence decay.[28] This will help in determining the "correct" extraction of energy transfer rates from the measurements.

Assessment of the model in the experimental context

We would like to conclude this discussion of experimental results with a brief review of the suitability of the optical model described in the ESI† to analyse and predict FRET signals and conformational change. We have seen that the energy transfer model based on rate equations uses only a small set of parameters that are easily accessible to measurement. The absorption cross sections can be obtained from transmission measurements, the decay rates from fluorescence decay measurements. The energy transfer rate is gained from a comparison between proteins taking part in energy transfer and proteins without energy transfer, as is customary for these systems. The model describes well the features encountered in FRET systems, namely changes in the emission intensity of donors and acceptors and changes in apparent decay rates caused by the energy transfer. The model proved its predictive quality in the quantitative analysis of the acceptor fluorescence decay. With the set of parameters derived from our data, the scope of the model can be widened to include optical response to changes in concentration of the binding species, a feature of particular interest *e.g.* in biosensor applications. Further, the model proved valuable in tracing conformational changes of the FRET protein over time. This is a first step in the direction of automated, real-time monitoring of drug–protein interactions and their time constants.

The model as described in the ESI† is generic in the sense that it allows for different donor and acceptor concentrations and thus in principle applies to all systems with energy transfer in which the donor and the acceptor can be described by two level systems. In the case of CFP–GBP–YFP, which we analysed in this article, the concentrations of the donor and acceptor are equal. This reduces the complexity of the calculations.

Beyond the scope of the model, however, is the description of the proteins from an *ab initio* molecular and electronic perspective, notwithstanding the fact that the energy transfer in principle allows the determination of the distance between donor and acceptor proteins. The model is based on the assumption that the emission of fluorescence photons is stochastically independent, thus it is challenged in dealing with non-single exponential behaviour. The non-single exponential decays make the definition of a single decay rate difficult. However, as soon as the physical origin and the molecular implications of the multiple exponential decays are clear, the flexibility inherent in the model allows easy inclusion of these kinetic details. The ambiguity in the donor decay rate is currently the major challenge in connecting the optical properties of any CFP-based FRET protein with its mechanical properties and conformation. Progress in this area is expected once the description of the fluorescent proteins has gained an analytical photochemical foundation. Alternatively, the ambiguity is avoided in newly synthesized FRET systems with single exponential fluorescence decays in both the donor and acceptor, such as Cerulean variants.[41]

Overall, our model appears valuable as an empirical means to describe the behaviour of FRET proteins. Its excellent description of the kinetic properties of energy transfer pardons the one or other heroic assumption on which it is based, such as the assumed independency of the intrinsic CFP decay rate from the molecular environment. As an empirical tool, it may help in the estimate of optical output power from a biosensor utilising these proteins and in the analysis of biosensor signals, as well as in the determination of time constants of binding/release reactions of proteins of interest.

Conclusions

We investigated the optical properties of the CFP–GBP–YFP protein, where CFP and YFP are linked to a central functional GBP group. CFP and YFP act as a FRET pair, whose fluorescence provides details on the structure and conformation of the central group. In the given construct, CFP acts as an energy donor and YFP as an acceptor, while the GBP acts as a molecular switch whose conformation is dependent on whether its binding site for Ca^{2+} is occupied or not. Conformational changes following Ca^{2+} binding or release result in a decrease or increase of the distance between CFP and YFP and consequently lead to a conformation-dependent efficiency of energy transfer between the two fluorescent protein moieties and a corresponding change in FRET.

We investigated steady-state as well as dynamic optical properties of the FRET protein and compared them to the corresponding properties of the free fluorescent proteins CFP and YFP. Transmission measurements showed that the absorption cross sections of the fluorescent proteins are affected by their fusion to GBP. Values obtained on free proteins therefore do not represent the real absorption cross sections of chimaeric FRET constructs as investigated here. However, absorption and fluorescence spectra of CFP–GBP–YFP can be precisely described by weighted sums of the corresponding spectra of the free fluorescent proteins, indicating that the optical properties of CFP–GBP–YFP are dominated by those of its fluorescent moieties. Consequences of energy transfer between CFP and YFP in the FRET protein can be identified both in steady state fluorescence measurements as well as in fluorescence decay measurements. The latter, in particular, provide a tool well-suited for tracing the flow of energy through the FRET system. Finally, we were able to track conformational changes of the GBP protein in response to binding and release of Ca^{2+} *via* observation of the changes in energy transfer efficiency. Observation and evaluation of either the steady-state fluorescence intensities or the fluorescence decays of the donor and acceptor allow determination of the time-dependence of Ca^{2+} binding and release.

To make the properties of CFP–GBP–YFP useful for application, we developed a simple optical model based on rate equations, which describes absorption, fluorescence and energy transfer and is able to reproduce all features in our dataset. The full set of parameters of the model was determined

from measurements reported in this article. Thus, the model can serve in predictive applications which are of advantage, for example, in the design of biosensors employing CFP–GBP–YFP or similar molecules.

Further, we were able to show that application of the rate equation model allows the observation of the conformational changes of GBP in CFP–GBP–YFP in a semi-quantitative manner. Important challenges on the way to complete quantitative evaluation of conformational changes *via* measurements of FRET between the fluorescent moieties were identified: linking the distance of the fluorescent proteins to the specific conformation of the central functional group, and an understanding of the multi-exponential fluorescence decay of CFP. However, we were able to show that in spite of these limitations, the measurement of energy transfer efficiency allows us to quantify the reaction time constants of analyte molecules with the FRET protein in real time.

Overall, the rate equation model developed in this article allows the treatment of both descriptive and predictive analyses involving energy transfer between fluorescent proteins in general and inside FRET proteins in particular. Naturally, the parameters of the model need to be re-determined for each FRET couple, and possibly each batch of a particular protein, to avoid misinterpretations of the results.

Acknowledgements

The authors are grateful for partial support of this work by the European Commission under contract number 031867—Integrated Project P. Cezanne and under grant agreement number 228334—Laserlab Europe II. They thank G. Sianidis for preliminary experiments and Benjamin Eckmans, Astrid Ziegler and Sarah Bardakji for their experimental support.

Notes and references

1 R. Y. Tsien, *Annu. Rev. Biochem.*, 1998, **67**, 509–544.
2 A. Prinz, G. Reither, M. Diskar and C. Schultz, *Proteomics*, 2008, **8**, 1179–1196.
3 S. Nowotschin, G. S. Eakinl and A. K. Hadjantonakis, *Trends Biotechnol.*, 2009, **27**, 266–276.
4 H. W. Detrich 3rd, *Methods Cell Biol.*, 2008, **85**, 219–241.
5 R. H. Berg and R. N. Beachy, *Methods Cell Biol.*, 2008, **85**, 153–177.
6 D. M. Kwinter and M. A. Silverman, *J. Vis. Exp.*, 2009, May 29 (27).
7 L. Yan, Y. Han, Y. He, H. Xie, J. Liu, L. Zhao, J. Wang, L. Gao and D. Fan, *Stem Cell Rev. Rep.*, 2007, **3**, 265–269.
8 G. Yang and S. G. Withers, *ChemBioChem*, 2009, **73**, 1251–1258.
9 S. T. Hau, G. Blaser and S. E. Jackson, *Chem. Soc. Rev.*, 2009, **38**, 2951–2965.
10 K. Yagi, *Appl. Microbiol. Biotechnol.*, 2007, **73**, 1251–1258.
11 A. Ibraheem and R. E. Campbell, *Curr. Opin. Chem. Biol.*, 2010, **14**, 30–36.
12 S. B. VanEngelenburg and A. E. Palmer, *Curr. Opin. Chem. Biol.*, 2008, **12**, 60–65.
13 H. J. Carlson and R. E. Campbell, *Curr. Opin. Biotechnol.*, 2009, **20**, 19–27.
14 P. R. Selvin, *Nat. Struct. Biol.*, 2000, **7**, 730–734.
15 C. L. Takanishi, E. A. Bykova, W. Cheng and J. Zheng, *Brain Res.*, 2006, **1091**, 132–139.
16 T. Förster, *Ann. Phys.*, 1948, **6**, 55–75.
17 S. Pelet, M. J. R. Previte and P. T. C. So, *J. Biomed. Opt.*, 2006, **11**, 1–11.
18 F. Ciruela, *Curr. Opin. Biotechnol.*, 2008, **19**, 338–343.
19 R. Grailhe, F. Merola, J. Ridard, S. Couvignou, C. Le Poupon, J.-P. Changeux and H. Laguitton-Pasquier, *ChemPhysChem*, 2006, **7**, 1442–1454.
20 T. C. Voss, I. A. Demarco and R. N. Day, *BioTechniques*, 2005, **38**, 413–424.
21 T. Niittylae, B. Chaudhuri, U. Sauer and W. B. Frommer, *Methods Mol. Biol.*, 2009, **553**, 355–372.
22 D. Kajihara, R. Abe, I. Iijima, Ch. Komiyama, M. Sisido and T. Hohsaka, *Nat. Methods*, 2006, **3**, 923–929.
23 L. Alvarez, Ch. Houée Levin, F. Merola, T. Bizouarn, H. Pasquier, L. Baciou, F. Rusconi and M. Erard, *Photochem. Photobiol.*, 2010, **86**, 55–61.
24 T. Förster, C. Strohhöfer, K. Bock, P. Kasak, M. Danko, Z. Kronekova, T. Nedelcev, I. Krupa and I. Lacík, *Transducers '09, Int. Conf. Solid-State Sens., Actuators Microsyst.*, 2009, 1218–1221.
25 K. Ye and J. S. Schultz, *Anal. Chem.*, 2003, **75**, 3451–3459.
26 E. B. van Munster and T. W. Gadella, *Adv. Biochem. Eng./Biotechnol.*, 2005, **95**, 143–175.
27 A. G. Harpur, F. S. Wouters and P. I. H. Bastiaens, *Nat. Biotechnol.*, 2001, **19**, 167–169.
28 A. Villoing, M. Ridhoir, B. Cinquin, M. Erard, L. Alvarez, G. Vallverdu, P. Pernot, R. Grailhe, F. Mérola and H. Pasquier, *Biochemistry*, 2008, **47**, 12483–12492.
29 M. Millington, G. J. Grindlay, K. Altenbach, R. K. Neely, W. Kolch, M. Benčina, N. D. Read, A. C. Jones, D. T. F. Dryden and S. W. Magennis, *Biophys. Chem.*, 2007, **127**, 155–164.
30 J. W. Borst, M. A. Hink, A. van Hoek and A. J. W. G. Visser, *J. Fluoresc.*, 2005, **15**, 153–160.
31 M. Jose, D. K. Nair, C. Reissner, R. Hartig and W. Zuschratter, *Biophys. J.*, 2007, **92**, 2237–2254.
32 M. Tramier, I. Gautier, T. Piolot, S. Ravalet, K. Kemnitz, J. Coppey, Ch. Durieux, V. Mignotte and M. Coppey-Moisan, *Biophys. J.*, 2002, **83**, 3570–3577.
33 M. H. J. Seifert, *J. Am. Chem. Soc.*, 2002, **124**, 7932–7942.
34 M. Tramier, K. Kemnitz, C. Durieux and M. Coppey-Moisan, *J. Microsc.*, 2004, **213**, 110–118.
35 G. Patterson, R. N. Day and D. Piston, *J. Cell Sci.*, 2001, **114**, 837–838.
36 Ref. 31 determines the radiative rates of eCFP and eYFP from Strickler–Berg analysis. The rates (2×10^8 s^{-1} for eCFP and 1.4×10^8 s^{-1} for eYFP) differ from the ones reported in this article. The reason for the discrepancy between results obtained by two different methods requires further investigation.
37 N. K. Vyas, M. N. Vyas and F. A. Quiocho, *Nature*, 1987, **327**, 635–638.
38 S. D'Auria, A. Ausili, A. Marabotti, A. Varriale, V. Scognamiglio, M. Staiano, E. Bertoli, M. Rossi and F. Tanfani, *J. Biochem.*, 2006, **139**, 213–221.
39 P. Herman, J. Vecer, I. Barvik Jr., V. Scognamiglio, M. Staiano, M. de Champdoré, A. Varriale, M. Rossi and S. D'Auria, *Proteins: Struct., Funct., Bioinf.*, 2005, **61**, 184–195.
40 G. H. Patterson, D. W. Piston and B. George Barisas, *Anal. Biochem.*, 2000, **284**, 438–440.
41 M. A. Rizzo, G. H. Springer, B. Granada and D. W. Piston, *Nat. Biotechnol.*, 2004, **22**, 445–449.